

On Forced Oscillations in a Relay System with Hysteresis

Zh. T. Zhusubaliyev^{*,a}, U. A. Sopuev^{**b}, and D. A. Bushuev^{***c}

^{*}Southwest State University, Kursk, Russia

^{**}Osh State University, Osh, Kyrgyzstan

^{***}Belgorod State Technological University named after V.G. Shukhov, Belgorod, Russia

e-mail: ^azhanybai@gmail.com, ^bulansopuev@mail.ru, ^cuntame@list.ru

Received June 22, 2023

Revised February 26, 2024

Accepted March 4, 2024

Abstract—This paper discusses the phenomenon associated with the forced synchronization (“entrainment of a self-sustained oscillator by an external force”) in a relay system with hysteresis, which manifests itself in the occurrence of periodic motions close to the rhythmic activity of neurons, when packets of fast oscillations are interspersed with intervals of the slow dynamics.

To study this phenomenon, we introduce a circle mapping, which, depending on the parameters, can be a circle diffeomorphism or discontinuous map (“gap map”). In both cases, this mapping demonstrates the so-called period-adding bifurcation structure.

It is demonstrated that packets number of fast oscillations in the period of periodic motion is determined by the rotation number, and the length of the intervals between the packets may be found of the boundaries of the absorbing interval. The change in the number of pulses in the packet occurs through the border-collision bifurcation.

Keywords: forced relay system with hysteresis, system with two time scales, discontinuous circle mapping, border-collision and period adding bifurcations

DOI: 10.31857/S0005117924040059

1. INTRODUCTION

Let us consider the relay system with hysteresis [1–3] and external periodic action. The behavior of this system is described by a differential equation

$$\dot{x} = f(t, x), \quad f(t, x) = \lambda(x - S(x, \eta) + \sigma(t)), \quad \sigma(t + \pi) = -\sigma(t). \quad (1)$$

Here t is the time variable, x is an unknown function of t and f is a given function of t and x ($t, x, f \in \mathbb{R}$). \dot{x} is the derivative of x with respect to t and S is the output (switching function) signal of the relay element. The absolute value of λ is proportional to the time constant of the plant, and $\sigma(t) = \mu_0 + \mu_m \cos t$ is the forced signal, where μ_0, μ_m are the constant component and the amplitude of the variable component $\sigma(t)$, respectively.

The output signal S of the relay element is defined as

$$S(x, \eta) = \begin{cases} 1, & x < q - \chi, & q - \chi < x < q + \chi, & \eta = 1; \\ 0, & x > q + \chi, & q - \chi < x < q + \chi, & \eta = 0. \end{cases}$$

Here q is the setting signal; χ is the hysteresis of a relay element; $\eta = 0, +1$ are the values of the function S after the previous switching of the relay element.

As can be seen from equation (1), the right part depends on both t and x . The function f periodically changes by t with a period of 2π . In addition, the function $x(t)$ satisfying (1) is invariant with respect to the shift of the origin of t by 2π [4].

Parameters: $\lambda = -7.5/\pi$, $q = 4.0/\Gamma$; $\mu_0 = 1.5/\Gamma$; $\mu_m = 0.525/\Gamma$; $\chi = \chi_0/\Gamma$. In the following bifurcation analysis, we shall consider Γ and χ_0 as control parameters: $6.0 \leq \Gamma \leq 7.0$, $0.35 \leq \chi_0 \leq 0.65$.

Differential equations of the form (1) are used to study many problems of engineering, mechanics, physics [5–7], and biology.

Examples in biology include the analysis of one particular type of cardiac arrhythmia, atrioventricular conduction block [8–10], investigations of biological mechanisms for sleep-wake regulation [11–14], the study rhythmic activity of neurons [15–21].

In [22] it was shown that with accepted idealizations, a mathematical model of a vibration machine with unbalanced excitation of vibrations and relay control can be reduced to the equation (1).

The considered class of relay systems refers to systems with two time scales (for example see [23, 24]), the dynamics of which are determined by two frequencies: high frequency oscillations generated by fast switchings of the relay element modulated by the low-frequency reference signal.

Such systems demonstrate a phenomenon close to the rhythmic activity of neurons, when packets of fast oscillations are interspersed with intervals of the slow dynamics. A typical example of a model mapping describing this behavior of neurons is the discontinuous map of Rulkov [17] (see also the review [19]). The bifurcation mechanisms of the occurrence of such oscillations have been studied by many authors (for example see [18–21, 25]).

In this paper, we study the entrainment of a self oscillations of the relay system with hysteresis by an external periodic signal, which manifests itself in the occurrence of regular motions close to the rhythmic dynamics of neurons.

First, we reduce the differential equation (1) to circle mapping. It is shown that, depending on the parameters, such a mapping is a circle diffeomorphism or discontinuous (“gap map”).

Next we obtain analytically the equation for the boundaries of the gap and boundaries of the absorbing interval in the phase space.

This allow us to obtain the boundary separating the domains of existence of a circle diffeomorphism and discontinuous map (“gap map”) in the parameter plane.

We found, that in both regions, the mapping demonstrates the so-called period-adding bifurcation structure [26, 27]. In [22], it was shown both numerically and experimentally that the intervals of low-frequency oscillations, are interrupted by bursts of fast oscillations.

In the present study is demonstrated that packets number of fast oscillations in the period of periodic motion is determined by the rotation number, and the length of the intervals between the packets may be found of the boundaries of the absorbing interval.

The change in the number of pulses in the packet occurs through the border-collision bifurcation when one of the points of the periodic orbit collides with the switching manifold. This corresponds to a collision solution of the equation (1) for $S = 1$ with the upper switching threshold of the relay element. Such a bifurcation in nonsmooth differential equations is called “grazing bifurcation” [28–31].

2. MATHEMATICAL MODEL IN DISCRETE TIME

2.1. Return Map

Due to the periodicity of f by t with a period of 2π , the phase plane (1) is a rectangle with a width of 2π with identified points N' , N (Fig. 1a). The equation (1) reduces to a system of autonomous differential equations

$$\dot{\theta} = 1, \quad \dot{x} = f(\theta, x), \quad (2)$$

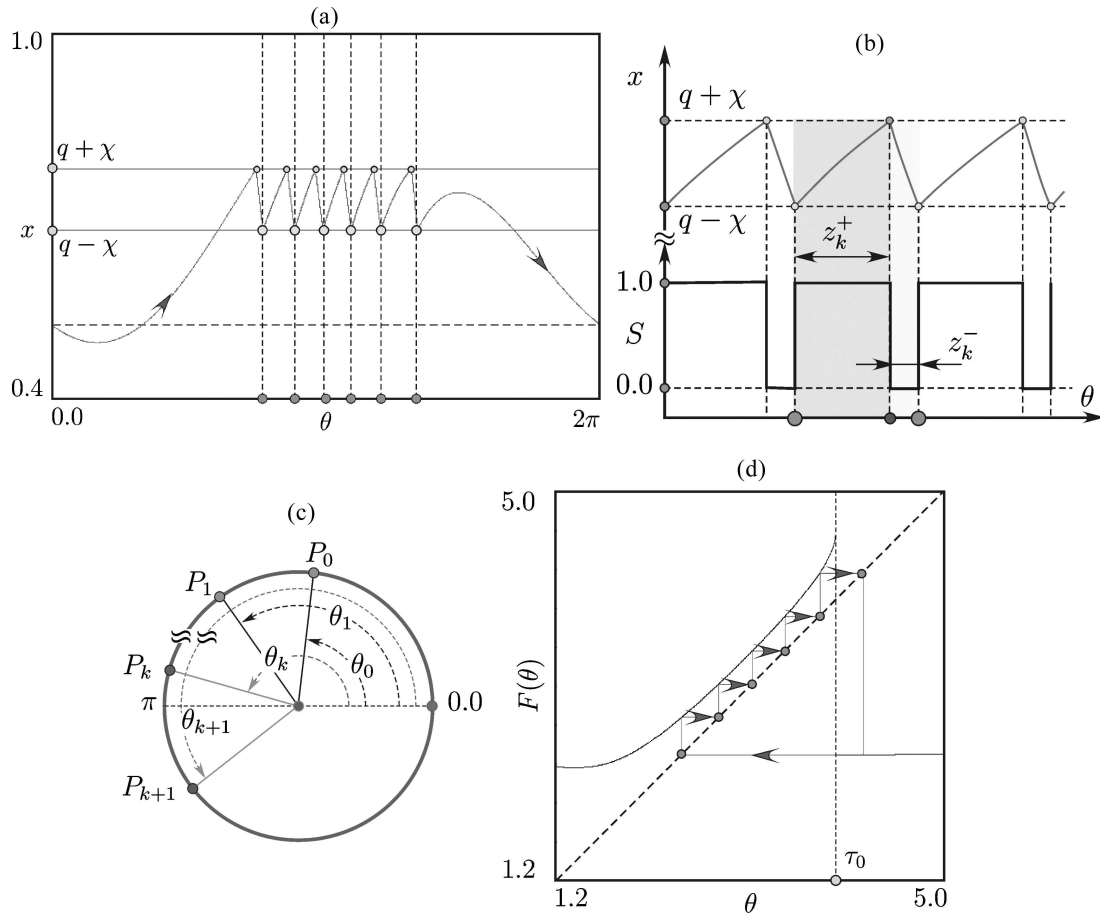


Fig. 1. (a) Periodic solution of a non-autonomous equation (1). (b) Magnified part of the periodic solution in (a), illustrating the technique of obtaining a mapping (3). (c) The mapping defined on the circle. (d) The periodic orbit of the mapping (3) corresponding to the periodic solution of the equation (1).

the phase variables of which are $\theta = t - 2\pi [t/(2\pi)]$ and x . Here $[\cdot]$ is the largest integer number not greater than argument (i.e., the integer part, or floor, of argument).

The solution to equation (2) starting at the point of the lower boundary $q - \chi$ of the hysteresis zone maps to the point located on the upper boundary $q + \chi$ then, after switching the relay element $S = 1 \rightarrow S = 0$, this point maps back to the lower boundary one (see Fig. 1b).

Let's connect the ends of the segment $[0; 2\pi]$ and form a circle of unit radius [1] (Fig. 1c). Then one can introduce a function F , which maps each point P_k on the unit circle into a point P_{k+1} , to which it will map P_k when rotated by an angle θ_{k+1} according to the differential equations (2) after a time $z_k^+ + z_k^-$, where z_k^\pm is the pulse width at $S = 1$ and $S = 0$, respectively (Figs. 1b and 1c).

Then the change of the angle between consecutive points is $P_k = P(1, \theta_k)$, $k = 0, 1, 2, \dots$ on the unit circle is described by

$$\theta \mapsto F(\theta) \bmod 2\pi, \quad F(\theta) = \theta + z^+(\theta) + z^-(\theta), \quad 0, 0 \leq \theta \leq 2\pi. \tag{3}$$

Here z^+ is the smallest non-negative solution of the equation

$$q + \chi = e^{\lambda z^+} (q - \chi - 1 + \mu_0) + 1 - \mu_0 + A_m (\sin(\theta + z^+) - \lambda \cos(\theta + z^+)) - A_m e^{\lambda z^+} (\sin \theta - \lambda \cos \theta),$$

and z^- :

$$q - \chi = e^{\lambda z^-} (q + \chi + \mu_0) - \mu_0 + A_m (\sin(\theta' + z^-) - \lambda \cos(\theta' + z^-)) - A_m e^{\lambda z^-} (\sin \theta' - \lambda \cos \theta'), \quad A_m = \frac{\lambda \mu_m}{1 + \lambda^2}, \quad \theta' = \theta + z^+.$$

Hence the orbit of the point θ_0

$$\theta_1 = F(\theta_0), \theta_2 = F(\theta_1) = F^2(\theta_0), \dots, \theta_k = F^k(\theta_0), \dots$$

The nature of the dynamics on a circle is determined by the rotation number

$$r = \lim_{k \rightarrow \infty} \frac{F^k(\theta) - \theta}{2\pi k}.$$

If the rotation number is rational $r = \frac{n}{m}$, where n, m ($m \neq 0$) are integers, then there exists θ_0 such that

$$F^m(\theta_0) = \theta_0 \text{ mod } 2\pi$$

and the orbit on the circle is m -periodic.

If r is an irrational number, then, in the case of diffeomorphism, the dynamics is quasiperiodic: each iteration of the mapping gives a new point on the unit circle and none of these points repeats. Then P_k forms a dense set on the circle.

This was related to the properties of diffeomorphisms. If the mapping is noninvertible or discontinuous, then the specified properties are preserved, but there are differences. A detailed discussion of these differences can be found in [26].

To describe the orbit of the system (3) starting at the point θ_0 , one can use two characters \mathcal{L} and \mathcal{R} ("left," "right") [26]. Then the orbit $\mathcal{O}(\theta_0) = \{\theta_i = F^i(\theta_0), i = 0, 1, 2, \dots\}$ is described by the sequence:

$$\bar{\sigma}_0 \bar{\sigma}_1 \bar{\sigma}_2 \dots, \tag{4}$$

where the symbol $\bar{\sigma}_i, i = 0, 1, 2, \dots$ in this sequence for each $i \geq 0$ is defined as

$$\bar{\sigma}_i = \begin{cases} \mathcal{L}, & \theta_i < c_0; \\ \mathcal{R}, & \theta_i > c_0. \end{cases}$$

For one-dimensional maps with a single point of discontinuity, the rotation number r of the periodic orbit of the period m

$$\mathcal{O}_m(\theta) = \{\theta \in I : \theta, F^k(\theta), k = 1, \dots, m - 1\}, \\ F^m(\theta) = \theta, F^k(\theta) \neq \theta$$

is defined as [26]

$$r = \frac{N_{\mathcal{R}}(\mathcal{O}_m)}{N_{\mathcal{L}}(\mathcal{O}_m) + N_{\mathcal{R}}(\mathcal{O}_m)},$$

where $N_{\mathcal{L}}(\mathcal{O}_m), N_{\mathcal{R}}(\mathcal{O}_m)$ is a number of symbols \mathcal{L} and \mathcal{R} in equation (4).

2.2. Properties of the Mapping

- Let's rewrite the map (3) as

$$\theta_{k+1} = F(\theta_k),$$

$$F(\theta) = \begin{cases} F_{\mathcal{L}}(\theta), & \theta < c_0; \\ F_{\mathcal{R}}(\theta), & \theta > c_0. \end{cases}$$

The functions $F_{\mathcal{L}}$, $F_{\mathcal{R}}$ are continuous and strictly increase on the segments $[F_{\mathcal{R}}(c_0); c_0]$ and $[c_0; F_{\mathcal{L}}(c_0)]$, respectively. The F mapping has no fixed points in $(F_{\mathcal{R}}(c_0); F_{\mathcal{L}}(c_0))$.

- If

$$F_{\mathcal{R}} \circ F_{\mathcal{L}}(c_0) < F_{\mathcal{L}} \circ F_{\mathcal{R}}(c_0),$$

then each point $\theta \in J$ has either a single preimage, or has no preimages inside J .

If there is a non-empty subinterval $(F_{\mathcal{R}} \circ F_{\mathcal{L}}(c_0); F_{\mathcal{L}} \circ F_{\mathcal{R}}(c_0))$ consisting of points that have no preimages in J , then in this case it is said that F is discontinuous ("gap map").

- Figure 2a shows the case when the F function is continuous and monotonically increasing. Then F contains one fictitious point of discontinuity such that

$$F_{\mathcal{R}}(c_0) = F_{\mathcal{L}}(c_0)$$

and $F(\theta + 2\pi) = F(\theta) + 2\pi$.

- Figure 2b shows the case when F contains a single point of discontinuity. How the gap occurs is explained below. Moreover, the points $c_{\mathcal{L}} = F_{\mathcal{R}}(c_0)$ and $c_{\mathcal{R}} = F_{\mathcal{L}}(c_0)$, called critical points of rank one, define the boundaries of the invariant absorbing interval $J = [c_{\mathcal{L}}; c_{\mathcal{R}}]$. The function F may have local extremes, but they are outside of J . Therefore, inside J , the function F is piecewise increasing.

Moreover, in this case $F_{\mathcal{L}}(c_0) < F_{\mathcal{R}}(c_0)$, so that in the absorbing interval J the mapping F is discontinuous ("gap map") (see Fig. 2c).

- The condition when the mapping F becomes discontinuous is formulated by the following Statement 1.

Statement 1. *A discontinuity F occurs when the solution $x(t)$ of the equation (1) for $S = 1$, starts at the point of the lower threshold $q - \chi$ switching of the relay element, tangents the upper threshold of switching $q + \chi$. In this case, the function F has a point of discontinuity c_0 , which satisfies the equation*

$$F(c_0) = c_*, \tag{5}$$

where $F(y) = y + z^+(y)$ [22, 27].

It is easy to see that the function Q on the right side of the equation (5) is given implicitly. Our goal is to obtain the equation with respect to the point of discontinuity c_0 explicitly.

The condition of tangency $x(t)$ to the upper switching threshold of the relay element is written as

$$\varphi_t + \varphi_x \dot{x}(t)|_{t=c_*} = 0, \quad \varphi = q + \chi - x. \tag{6}$$

Since $\varphi_t = 0$ and $\varphi_x = -1$, then (6) is equivalent to

$$\dot{x}(t)|_{t=c_*} = 0, \quad \dot{x} = \lambda(x - 1 + \mu_0 + \mu_m \cos t).$$

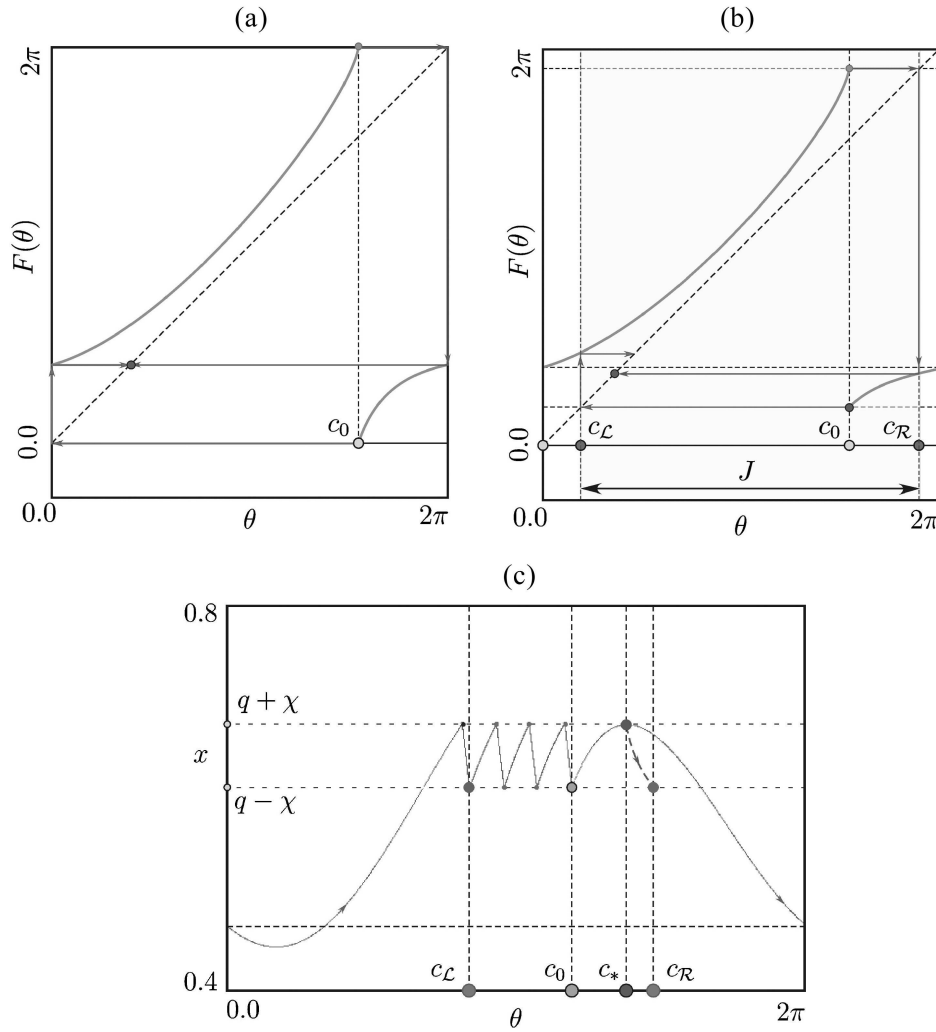


Fig. 2. (a) Circle diffeomorphism. (b) Discontinuous map (“gap map“). (c) Determination of the discontinuity point F and boundaries of the absorbing interval J .

Hence

$$x(c_*) - 1 + \mu_0 + \mu_m \cos c_* = 0.$$

Taking into account that $x(c_*) = q + \chi$, we get

$$q + \chi - 1 + \mu_0 + \mu_m \cos c_* = 0.$$

By solving this equation with respect to c_* , we have

$$c_* = 2\pi - \arccos\left(\frac{1 - q - \chi - \mu_0}{\mu_m}\right),$$

if $-1 \leq \frac{1 - q - \chi - \mu_0}{\mu_m} \leq +1$.

From the condition $-1 \leq \frac{1 - q - \chi - \mu_0}{\mu_m} \leq +1$, we find the boundary L separating the regions of existence of a discontinuous map and a circle diffeomorphism in the parameter space. Let's denote these domains as Π_{span} and Π_{circle} . The boundary between Π_{gap} and Π_{circle} on the parameter plane (χ_0, Γ) is

$$L = \{(\chi_0, \Gamma) : \Gamma = 6.025 + \chi_0\}. \tag{7}$$

After c_* is found, we determine the point of discontinuity c_0 . To obtain the equation with respect to c_0 explicitly, we use the tangency condition

$$x(c_*) - 1 + \mu_0 + \mu_m \cos c_* = 0. \quad (8)$$

Since

$$\begin{aligned} x(c_*) &= e^{\lambda(c_*-c_0)}(q - \chi - 1 + \mu_0) + 1 - \mu_0 \\ &+ A_m t(\sin c_* - \lambda \cos c_*) - A_m e^{\lambda(c_*-c_0)}(\sin c_0 - \lambda \cos c_0), \end{aligned} \quad (9)$$

then, substituting (9) into (8), we get:

$$\begin{aligned} e^{\lambda(c_*-c_0)}(q - \chi - 1 + \mu_0) + A_m(\sin c_* - \lambda \cos c_*) \\ - A_m e^{\lambda(c_*-c_0)}(\sin c_0 - \lambda \cos c_0) + \mu_m \cos c_* = 0. \end{aligned}$$

This equation is solved numerically.

3. BIFURCATION ANALYSIS

Figure 3a presents the two-dimensional bifurcation diagram in the (χ_0, Γ) parameter plane. Boundary L (7) separates the domains Π_{circle} and Π_{gap} .

Below the boundary of L (within the domain of Π_{circle}), the mapping (2) is a circle diffeomorphism, and the region Π_{gap} corresponds to the region of existence of a discontinuous mapping (“gap map”).

Figure 3b shows a bifurcation diagram obtained for the scan A in Fig. 3a: $0.4 \leq \chi_0 \leq 0.61$, $\Gamma = 6.6$ and Fig. 3c is a magnification of that part of this diagram, illustrating the transition to and from the synchronization 1 : 5 through the saddle-node bifurcation in Π_{circle} . Here dotted lines correspond to the unstable 5-cycle and solid lines to the stable one. At the boundaries of the resonant tongue with 1 : 5 stable and saddle 5-cycles merge and disappear.

Resonance domains have a classical structure, the so-called Arnold tongues. Between each two quasiperiodic regimes with different rotation numbers there exists a region of resonance dynamics.

Figure 3d presents a magnified part of the diagram in Fig. 3b illustrating the transition when we cross the boundary between the regions Π_{circle} and Π_{gap} . As you can see from this diagram, entering synchronization mode with 2 : 9 occurs in Π_{circle} , and the transition from the synchronization mode 2 : 9 occurs in the domain Π_{gap} .

Studies have shown that transitions at the left boundary of the tongue with 2 : 9 occur through the classical saddle-node bifurcation. In [22] it was shown that in the domains Π_{gap} such transitions are associated with border-collision fold bifurcation.

Figure 3e illustrates the so-called “Devil’s staircase”: the dependence of the rotation number r on χ_0 . In this figure, the plateaux correspond to the resonance tongues with 1 : 6, 1 : 5, 2 : 9 1 : 4. In Fig. 3f displays the bifurcation diagram for Π_{gap} , which demonstrates a sequence of period-adding bifurcations.

Finally, Fig. 4a shows periodic motion demonstrating the bursting dynamics in the Π_{gap} tongue with 1 : 6. As you can see from this figure, the number of packets with fast oscillations is determined by the numerator of the rotation number. The interval between the packets is determined by the boundaries of the absorbing interval. The change in the number of pulses in the packets occurs through the border-collision bifurcations, when one of the periodic points collides with the boundary of the gap F .

Periodic solution in the domain Π_{circle} is depicted in Fig. 4b, where this attractor is localized in the zone hysteresis of the relay element. The question is how to determine the characteristics of such behavior for Π_{circle} , remains open.

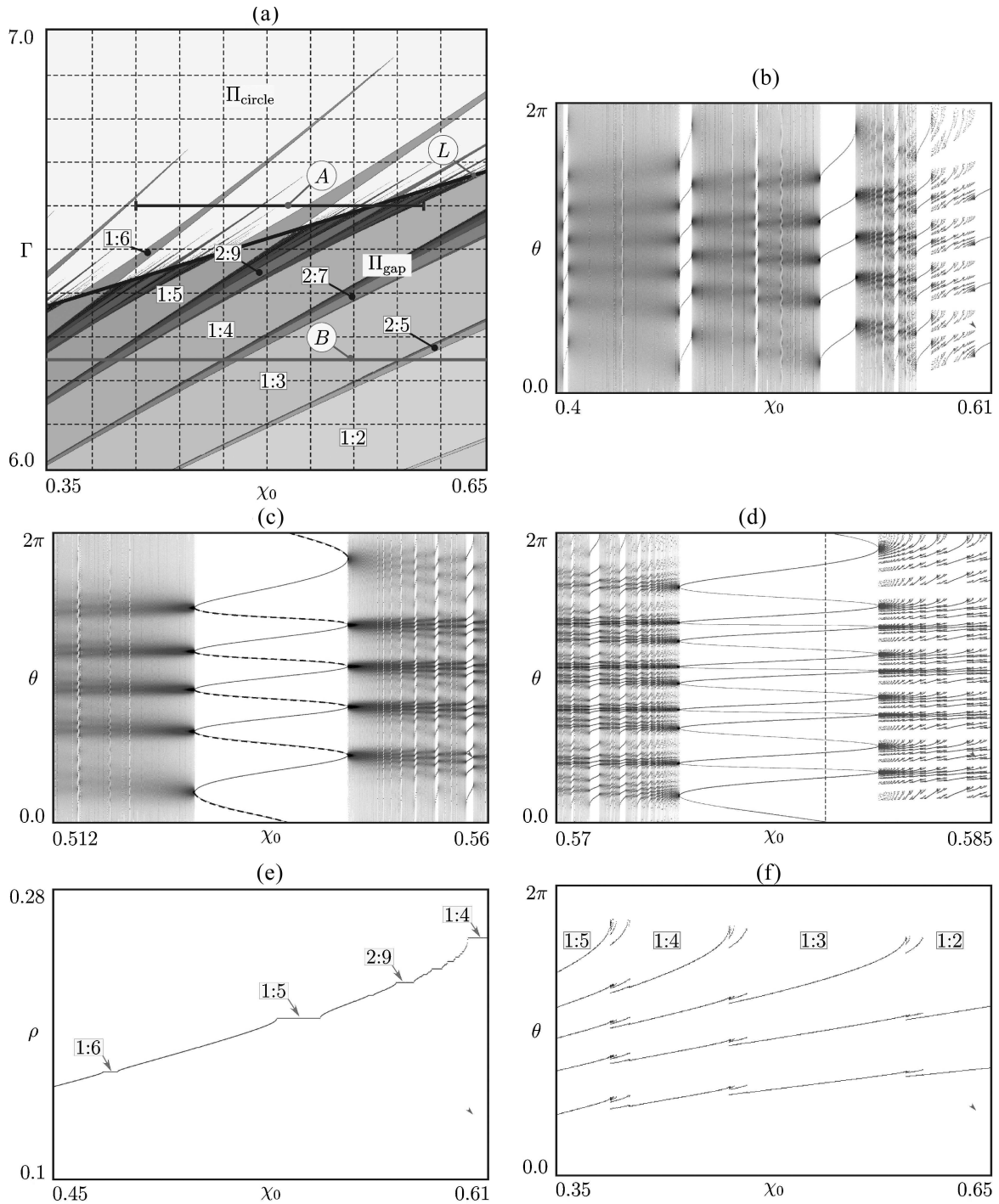


Fig. 3. (a) Bifurcation structure of the parameter plane (χ_0, Γ) of the map (3). The boundary L (7) separates the domains Π_{circle} and Π_{gap} in the parameter plane (χ_0, Γ) . (b) Bifurcation diagram for the scan A in (a) ($0.4 \leq \chi_0 \leq 0.61, \Gamma = 6.6$). (c) Magnified part of the bifurcation diagram in (b) near the tongue with 1:5 for Π_{circle} : ($0.512 \leq \chi_0 \leq 0.56, \Gamma = 6.6$). Here the dotted lines correspond to the unstable 5-cycle and solid lines to the stable one. (d) Magnified part of the bifurcation diagram in (b) for the neighborhood of the resonance 2:9, part of which is located in the region Π_{circle} , and part—in Π_{gap} . (scan A): $0.57 \leq \chi_0 \leq 0.585, \Gamma = 6.6$. (e) Devils staircase: dependence of the rotation number r on the parameter χ_0 , $0.45 \leq \chi_0 \leq 0.61, \Gamma = 6.6$. (f) Diagram for Π_{gap} , illustrating a sequence of the period adding bifurcations: $0.35 \leq \chi_0 \leq 0.65, \Gamma = 6.25$, (scan B).

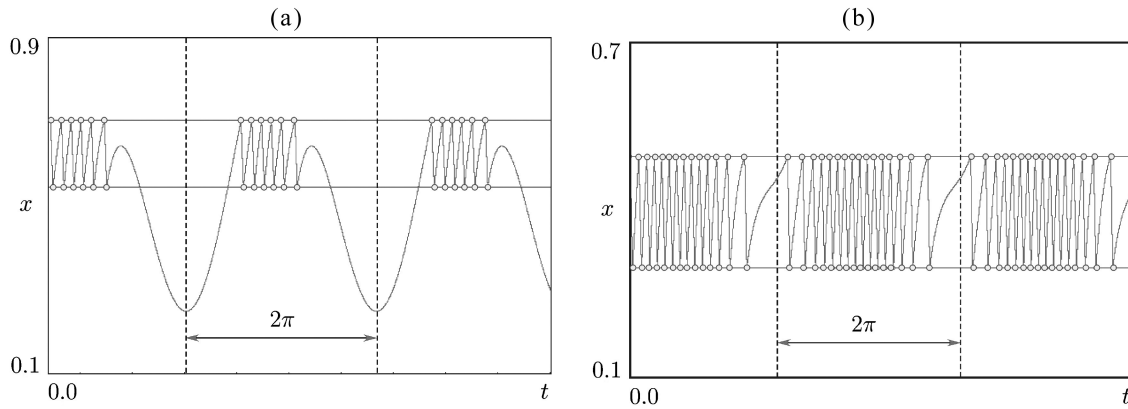


Fig. 4. (a) Periodic solution for Π_{gap} . (b) Periodic solution for Π_{circle} .

4. CONCLUSIONS

The paper was devoted to the discussion of an unusual phenomenon in a relay system with hysteresis and external periodic excitation. This phenomenon is associated with forced synchronization of relay systems and manifests itself in the occurrence of periodic dynamics close to the rhythmic activity of neurons, when packets of fast oscillations are interspersed with intervals of the slow dynamics.

To study this phenomenon, a circle mapping was introduced. Depending on the parameters, the mapping can be a circle diffeomorphizable or discontinuous map (“gap map”). It was shown that in both cases the mapping demonstrates the so-called period-adding bifurcation structure.

We found that in the Π_{gap} region, the number of packets with fast oscillations is determined in the period of periodic motion is determined by its rotation number, and the length of the intervals between packets is determined by the boundaries of the absorbing interval. The change in the number of pulses in a packet occurs through border-collision bifurcations, which in nonsmooth differential equations is called grazing bifurcations.

Due to the fact that the function F is piecewise monotonically increasing with one point of discontinuity c_0 in J (see Figs. 2a and 2b, the proof is given in [22]), Arnold tongues with rotation numbers $1:m$, $m = 2, 3, \dots$ (m is the cycle period) do not intersect on the parameter plane [7].

The regions of periodicity corresponding to stable m cycles of higher levels of complexity located between these tongues also do not overlap. The map (3) demonstrates the typical period adding phenomenon, and there can be no bistable behavior in one-dimensional maps of the class under consideration [7, 26, 32–34].

However, it is well known that if, for example, the function F increases to the left of the point of discontinuity, and decreases to the right one, then the bistability is possible [26]. In overlapped maps (“overlapping maps” [26]) the dynamics may be more complicated associated with multistability, as in multidimensional systems (see, for example, [35–38] and the the list of references there).

FUNDING

Zh.T. Zhusubaliyev was supported by the Ministry of Education and Science of the Russian Federation within the scope of the “Implementation of the Strategic Academic Leadership, program Priority 20302” (1.73.23 II; 1.7.21/S-2, 1.7.21/4-24-7). U.A. Sopuev was supported by the Osh State University (grants N 14-22; N 19-24). The work of D.A. Bushuev was supported within the framework of the Program “Priority-2030” using equipment of High Technology Center of the Belgorod State Technological University named after V.G. Shukhov.

REFERENCES

1. Neimark, Yu.I., *Metod tochechnykh otobrazhenii v teorii nelineinykh kolebaniy* (The Method of Point Maps in the Theory of Nonlinear Oscillations), Moscow: Nauka, 1972.
2. Tsyppkin, Ya.Z., *Relay Control Systems*, United Kingdom: Cambridge, University Press, 1984.
3. Gaushus, E.V., *Issledovanie dinamicheskikh sistem metodom tochechnykh preobrazovaniy* (Investigation of Dynamical Systems Using the Method of Point Maps), Moscow: Nauka, 1976.
4. Hale, J.K. and Koçak, H., *Dynamics and Bifurcations*, New York, Berlin, Heidelberg: Springer-Verlag, 1996.
5. Utkin, V.I., *Sliding Modes in Control Optimization*, Berlin, Germany: Springer-Verlag, 1992.
6. Filippov, A.F., *Differential Equations with Discontinuous Right-hand Sides*, Dordrecht, The Netherlands: Kluwer Academic Publishers, 1988.
7. Arnold, V.I., Small Denominators. I. Mappings of the Circumference onto Itself, *Am. Math. Soc. Transl. Ser. II*, 1965, vol. 46, pp. 213–284.
8. Arnold, V.I., Cardiac Arrhythmias and Circle Mappings, *Chaos*, 1991, vol. 1, no. 1, pp. 20–24.
9. Glass, L., Cardiac Arrhythmias and Circle Maps-A Classical Problem, *Chaos*, 1991, vol. 1, no. 1, pp. 13–19.
10. Keener, J.P., On Cardiac Arrhythmias: AV Conduction Block, *J. Math. Biol.*, 1981, vol. 12, pp. 215–225.
11. Borbély, A.A., Daan, S., Wirz-Justice, A., and Deboer, T., The Two-Process Model of Sleep Regulation: A Reappraisal, *J. Sleep Res.*, 2016, vol. 25, pp. 131–143.
12. Bailey, M.P., Derks, G., and Skeldon, A.C., Circle Maps with Gaps: Understanding the Dynamics of the Two-Process Model for SleepWake Regulation, *Eur. J. Appl. Math.*, 2018, vol. 29, pp. 845–868.
13. Derks, G., Glendinning, P.A., and Skeldon, A.C., Creation of Discontinuities in Circle Maps, *Proc. R. Soc. Lond. Ser. A Math. Phys. Eng. Sci.*, 2021, vol. 477, p. 20200872.
14. Şayli, M., Skeldon, A.C., Thul, R., Nicks, R., and Coombes, S., The Two-Process Model for SleepWake Regulation: A Nonsmooth Dynamics Perspective, *Physica D*, 2023, vol. 444, p. 133595.
15. Bressloff, P.C. and Stark, J., Neuronal Dynamics based on Discontinuous Circle Maps, *Phys. Lett. A*, 1990, vol. 150, nos. 3, 4, pp. 187–195.
16. Coombes, S., Thul, R., and Wedgwood, K.C.A., Nonsmooth Dynamics in Spiking Neuron, *Physica D*, 2012, vol. 241, pp. 2042–2057.
17. Rulkov, N.F., Modeling of Spiking-Bursting Neural Behavior Using Two-Dimensional Map, *Physical Review E*, 2002, vol. 65, no. 4, p. 041922.
18. Izhikevich, E.M., *Dynamical Systems in Neuroscience: The Geometry of Excitability and Bursting*, The Cambridge, Massachusetts: MIT Press, 2007.
19. Dmitrichev, A.S., Kasatkin, D.V., Klinshov, V.V., Kirillov, S.Yu., Maslennikov, O.V., Shchapin, D.S., and Nekorkin, V.I., Nonlinear Dynamical Models of Neurons, *Izvestiya VUZ. Applied Nonlinear Dynamics*, 2018, vol. 26, nos. 4–5, pp. 5–58.
20. Shilnikov, A.L. and Rulkov, N.F., Subthreshold Oscillations in a Map-Based Neuron Model, *Phys. Lett. A*, 2004, vol. 328, pp. 177–184.
21. Courbage, M., Nekorkin, V.I., and Vdovin, L.V., Chaotic Oscillations in a Map-Based Model of Neural Activity, *Chaos*, 2007, vol. 17, no. 4, p. 043109.
22. Zhusubaliyev, Zh.T., Avrutin, V., Rubanov, V.G., and Bushuev, D.A., Complex Dynamics of a Vibration Machine Caused by a Relay Feedback Control, *Physica D*, 2021, vol. 420, p. 32870.
23. Bi, Q.S., Chen, X.K., Kurths, J., and Zhang, Zh., Nonlinear Behaviors as Well as the Mechanism in a Piecewise-Linear Dynamical System with Two Time Scales, *Nonlinear Dynamics*, 2016, vol. 85, pp. 2233–2245.

24. Bi, Q.S. and Zhang, Zh., Bursting Phenomena as Well as the Bifurcation Mechanism in Controlled Lorenz Oscillator with Two Time Scales, *Phys. Lett. A*, 2011, vol. 375, pp. 1183–1190.
25. Turaev, D.V. and Shilnikov, L.P., Blue Sky Catastrophes, *Dokl. Math.*, 1995, no. 51, pp. 404–407.
26. Avrutin, V., Gardini, L., Sushko, I., and Tramontana, F., *Continuous and Discontinuous Piecewise-Smooth One-Dimensional Maps: Invariant Sets and Bifurcation Structures*, New Jersey, London, Singapore, Hong Kong: World Scientific, 2019.
27. Zhusubaliyev, Zh.T., Avrutin, V., Kucherov, A.S., Haroun, R., and El Aroudi, A., Period Adding with Symmetry Breaking/Recovering in a Power Inverter with Hysteresis Control, *Physica D*, 2023, vol. 444, p. 133600.
28. Nordmark, A., Non-Periodic Motion Caused by Grazing Incidence in an Impact Oscillator, *J. Sound Vibrat.*, 1991, vol. 145, no. 2, pp. 279–297.
29. Chin, W., Ott, E., Nusse, H.E., and Grebogi, C., Grazing Bifurcations in Impact Oscillators, *Physical Review E*, 1994, vol. 50, no. 6, pp. 4427–4444.
30. Di Bernardo, M., Feigin, M.I., Hogan, S.J., and Homer, M.E., Local Analysis of C-bifurcations in n -Dimensional Piecewise-Smooth Dynamical Systems, *Chaos, Solitons and Fractals*, 1999, vol. 19, no. 11, pp. 1881–1908.
31. Di Bernardo, M., Budd, C.J., Champneys, A.R., and Kowalczyk, P., *Piecewise-Smooth Dynamical Systems: Theory and Applications*, London: Springer-Verlag, 2008.
32. Keener, J.P., Chaotic Behavior in Piecewise Continuous Difference Equations, *Trans. Am. Math. Soc.*, 1980, vol. 261, no. 2, pp. 589–604.
33. Kaneko, K., On the Period-Adding Phenomena at the Frequency Locking in a One-Dimensional Mapping, *Prog. Theor. Phys.*, 1982, vol. 68, no. 2, pp. 669–672.
34. De Melo, W. and Van Strien, S., *One-Dimensional Dynamics*, New York: Springer, 1993.
35. Dudkowski, D., Czołczyński, K., and Kapitaniak, T., Multistability and Synchronization: The Co-Existence of Synchronous Patterns in Coupled Pendula, *Mechanical Systems and Signal Processing*, 2022, vol. 16, p. 108446.
36. Zhen Su, Zh., Kurths, J., Liu, Y., and Yanchuk, S., Extreme Multistability in Symmetrically Coupled Clocks, *Chaos*, 2023, vol. 33, p. 083157.
37. Kuznetsov, N., Mokaev, T., Ponomarenko, V., Seleznev, E., Stankevich, N., and Chua, L., Hidden Attractors in Chua Circuit: Mathematical Theory Meets Physical Experiments, *Nonlinear Dynamics*, 2023, vol. 111, pp. 5859–5887.
38. Zhusubalyev, Zh.T. and Mosekilde, E., Multistability and Hidden Attractors in a Multilevel Dc/Dc Converter, *Math. Comput. Simulat.*, 2015, vol. 109, pp. 32–45.

This paper was recommended for publication by N.V. Kuznetsov, a member of the Editorial Board